LNF-95/006

Inclusive Particle Photoproduction to Next-to-Leading Order

M. Greco, S. Rolli, A. Vicini

Zeitschrift Für Physik C 65, 277-284, (1995)

Z. Phys. C 65, 277–284 (1995)

ZEITSCHRIFT
FÜR PHYSIK C
© Springer-Verlag 1995

Inclusive particle photoproduction to next-to-leading order

M. Greco[1], S. Rolli[2], A. Vicini[3]

[1] Dipartimento di Fisica, Università dell'Aquila, and INFN, Laboratori Nazionali di Frascati, Frascati, Italy (e-mail: greco@lnf.infn.it)
[2] Dipartimento di Fisica Nucleare e Teorica, Università di Pavia, and INFN, Sezione di Pavia, Pavia, Italy, and NASA/Fermilab Astrophysics Center, FERMILAB, Batavia, Il 60510, USA (e-mail: rolli@fnalv.fnal.gov)
[3] Dipartimento di Fisica, Univeristà di Padova, and INFN, Sezione di Padova, Padova, Italy (e-mail: vicini@mvxpd5.pd.infn.it)

Received: 18 March 1994 / In revised form: 14 June 1994

Abstract. We study the inclusive photoproduction of neutral and charged pions and η at HERA, via the resolved photon mechanism, in QCD to next-to-leading order. We present various distributions of phenomenological interest and study the theoretical uncertainties due to the mass scales, and to photon and proton sets of structure functions. A new set of fragmentation functions for charged pions is also presented.

Inclusive production of high p_t particles and jets at HERA plays an important role in testing QCD, providing a detailed source of information on the hadron-like structure of the photon.

For this purpose leading order (LO) perturbative QCD predictions – based on evaluation of partonic cross sections at tree level and evolution of structure and fragmentation functions at one loop level– are not accurate enough, being plagued by the usual theoretical uncertainties associated to the large scale dependence of $O(\alpha_{em}\alpha_S)$ terms. A consistent calculation at next-to-leading order (NLO) needs two loop evolved structure and fragmentation functions and a NLO evaluation of parton-parton subprocesses.

As well known, two mechanisms contribute to the inclusive photoproduction of particles or jets at high energies: the photon can interact directly with the partons originating from the proton (direct process), or via its quark and gluon content (resolved process).

Previous theoretical analyses have considered both direct photoproduction to NLO, Aurenche et al. [1], and resolved photoproduction, Borzumati et al. [2], the latter having used the NLO corrections to all contributing parton-parton scattering processes of Aversa et al.[3] and LO fragmentation functions for the final hadron. Those results show the dominance of the resolved component at low p_t ($p_t < 10$ Gev), which is the region firstly explored at HERA, the role played by the direct contributions being shifted at higher p_t. The separation of the cross section in two components induces an artificial dependence on the photon factorization mass scale M_γ, which should cancel when the two terms are added up. Indeed this mechanism has been explicitly shown [4] to apply in the inclusive photoproduction of jets, which has been recently studied to NLO accuracy.

Motivated by these results, we consider in this paper the photoproduction of single hadrons in electron-proton collisions at HERA energies, based on the recent NLO fragmentation functions of ref. [5], limiting ourselves to the study of the resolved component only. A full NLO analysis including the direct term will be given elsewhere [6].

In particular we present a detailed quantitative evaluation of π^0, $\pi^\pm$ and η photoproduction at HERA at moderate p_t, using the hard scattering cross sections of ref. [3], and two loop structure and fragmentation functions. While the π^0 and η fragmentation functions have been discussed earlier [5, 7], a new set of NLO fragmentation functions for charged pions is presented here as well.

We give now the relevant formulae for the cross sections. The inclusive cross section for $ep \to h + X$ in an improved next-to-leading-order approximation is:

$$E_h \frac{d^3\sigma(ep \to h + X)}{d^3p_h} = \int_{x_{min}}^1 dx f_{\gamma/e}(x) \hat{E}_h \frac{d^3\hat{\sigma}(\gamma p \to h + X)}{d^3\hat{p}_h}(x) \tag{1}$$

where x_{min} is given in terms of the transverse momentum p_t and of the center-of-mass pseudorapidity η_{cm} of the produced hadron as:

$$x_{min} = \frac{p_t e^{\eta_{cm}}}{\sqrt{s} - p_t e^{-\eta_{cm}}} \tag{2}$$

The rapidity η_{lab} measured in the laboratory frame is related to η_{cm} as:

$$\eta_{lab} = \eta_{cm} - \frac{1}{2} \ln \frac{E_p}{E} \tag{3}$$

where E and E_p are the energies of the electron and the proton respectively ($E = 27$ GeV and $E_p = 820$ GeV, for the present HERA conditions).

The distribution in the longitudinal momentum fraction y of the outgoing photon has in the NLO approximation the following form [8]:

$$f_\gamma^{(e)}(y) = \frac{\alpha_{em}}{2\pi} \left\{ 2(1-y) \left[\frac{m_e^2 y}{E^2(1-y)^2\theta_c^2 + m_e^2 y^2} - \frac{1}{y} \right] \right.$$

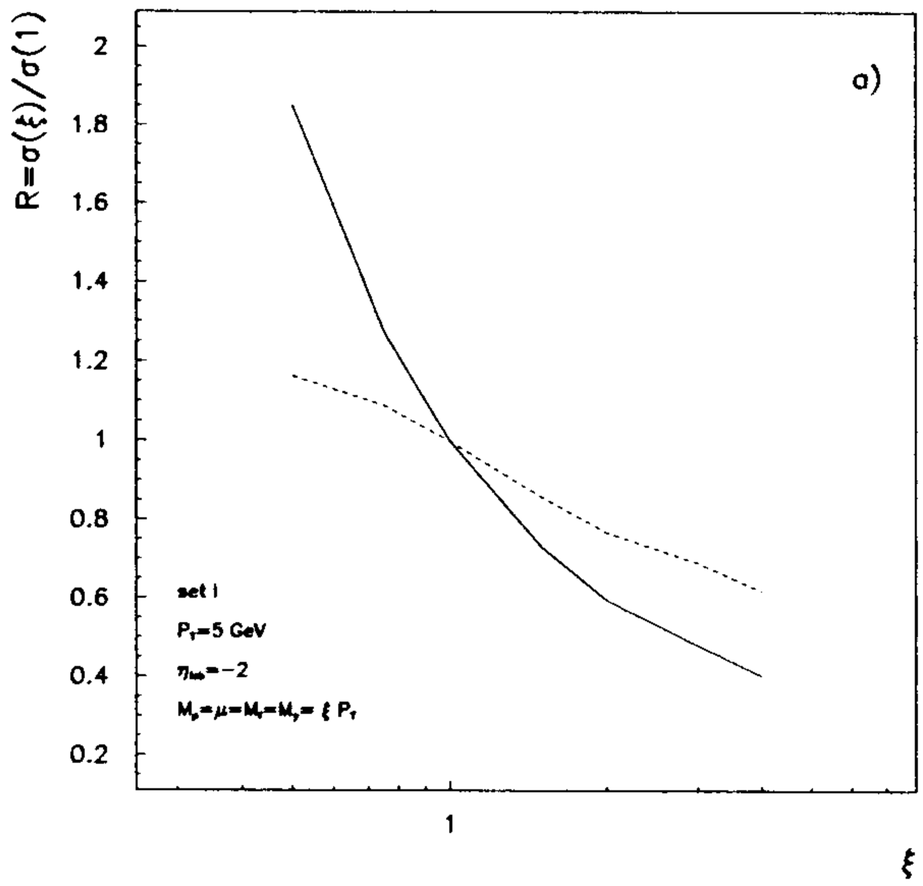

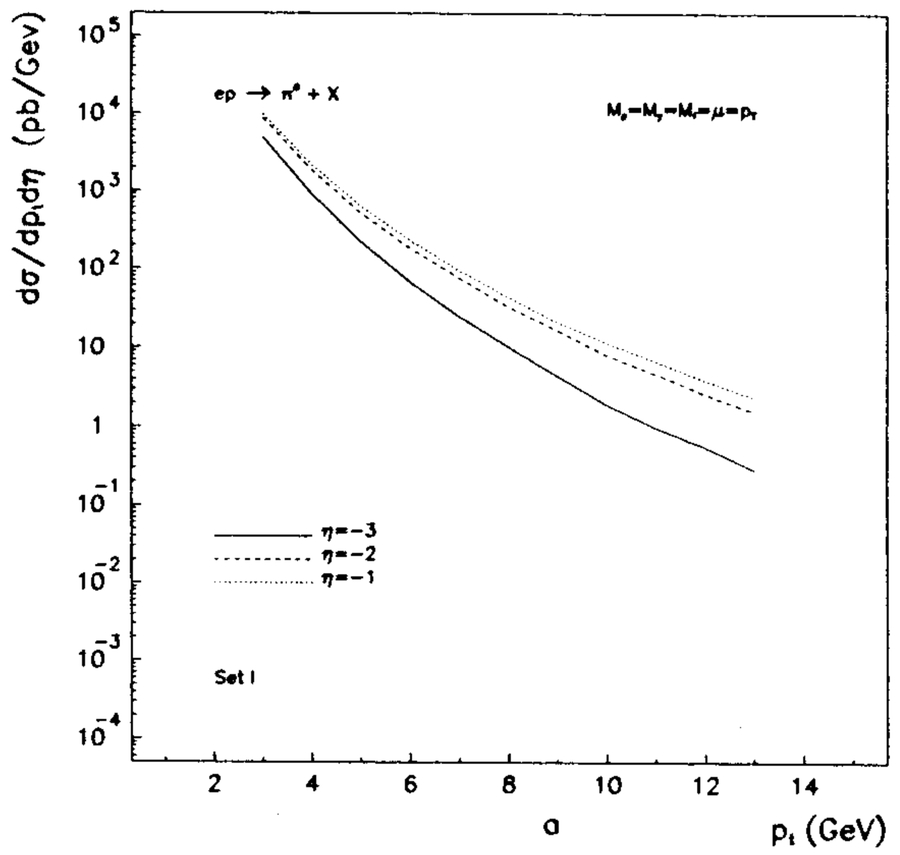

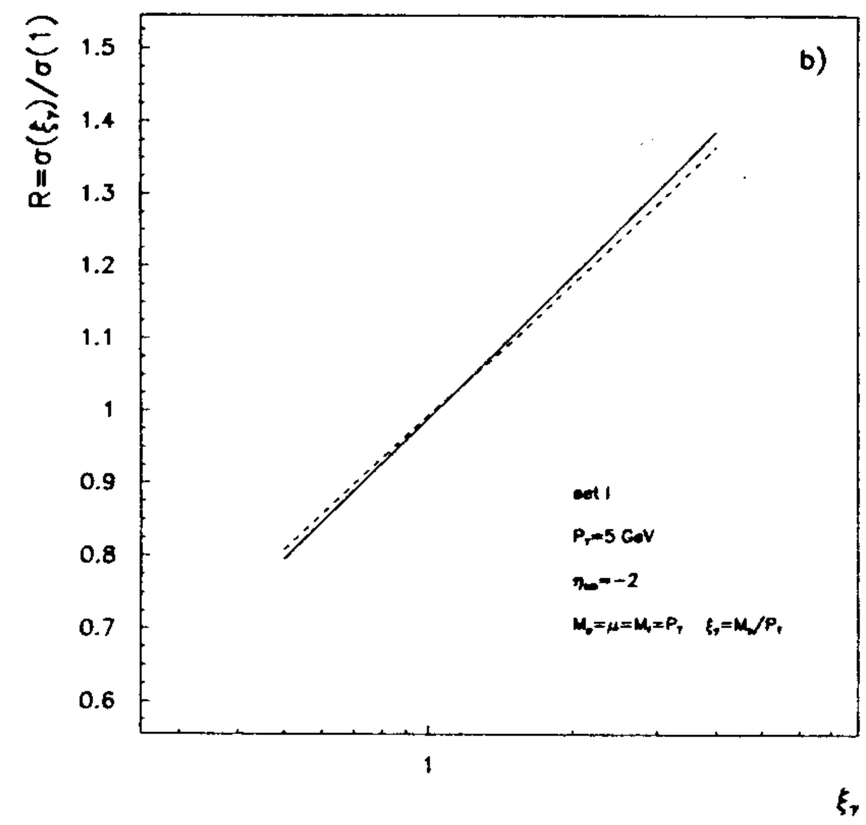

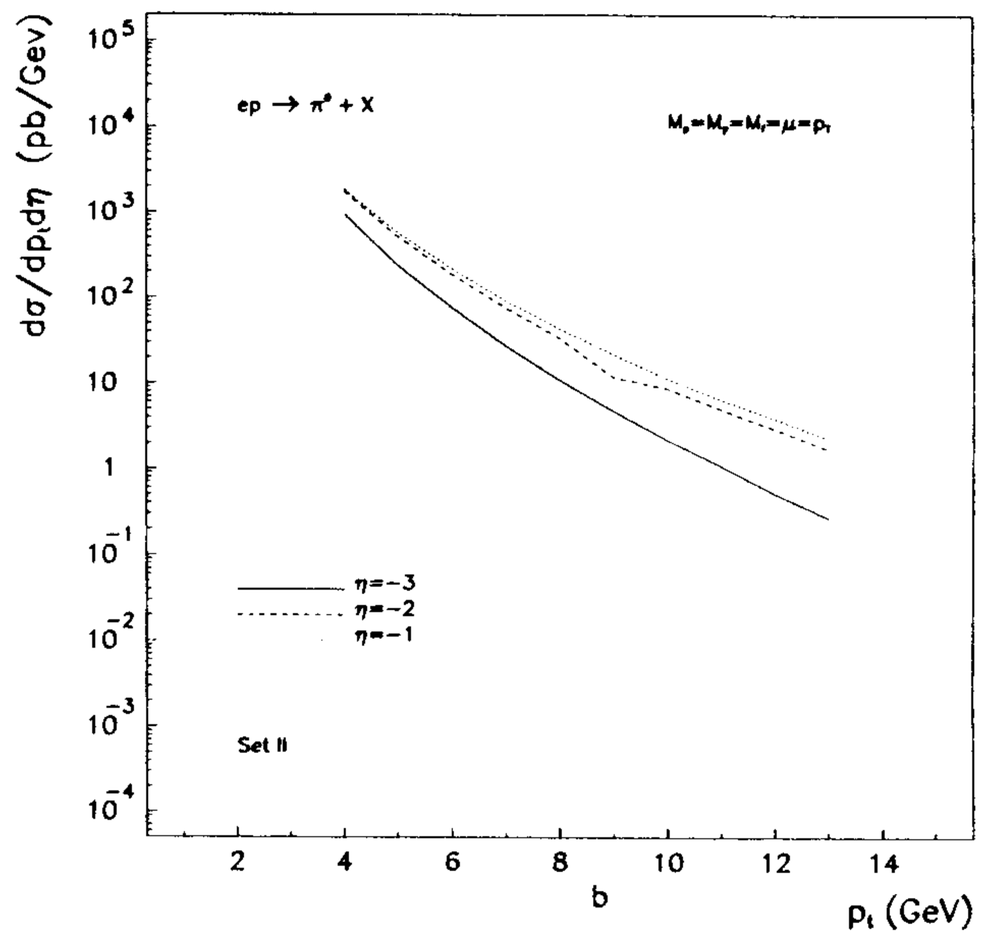

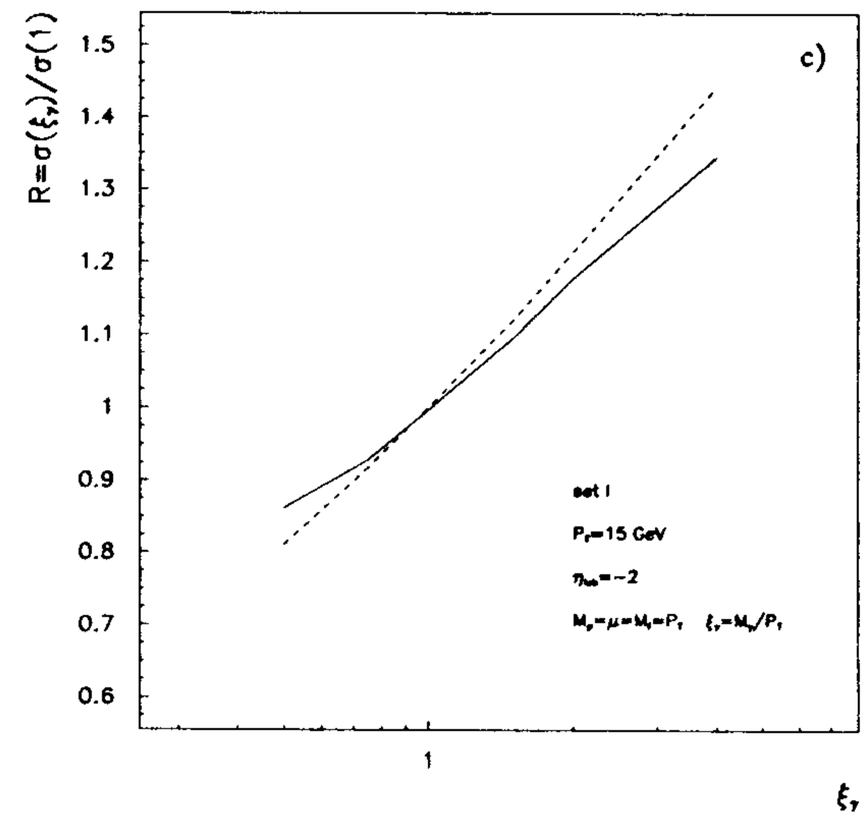

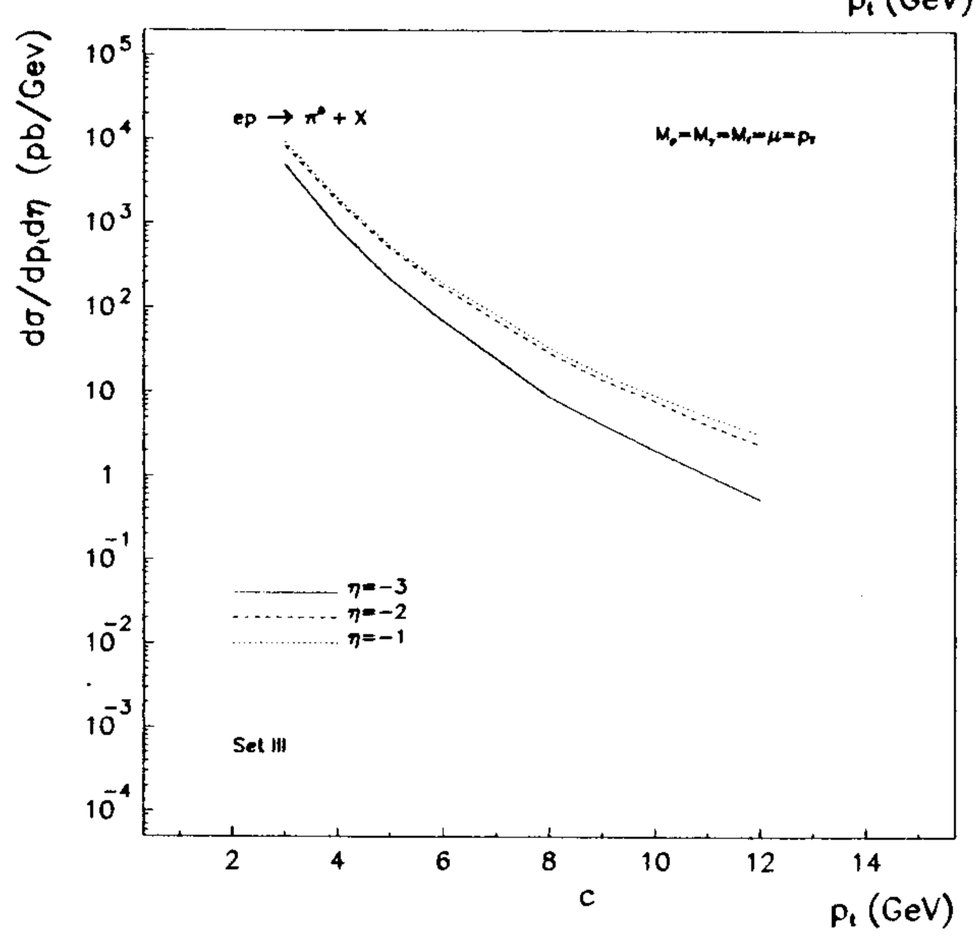

Fig. 1. π^0 production. Dependence of $\frac{d\sigma^{(ep)}}{d\eta dp_t}$ on the renormalization, factorization and fragmentation mass scales for $\eta_{lab} = -2$, **a)** $\mu = M_p = M_\gamma = M_f = \xi p_t$ for $p_t = 5$ GeV; **b)** $M_\gamma = \xi_\gamma p_t$ and $M_p = M_f = \mu = p_t$ and for $p_t = 5$ GeV; **c)** same as b) but for $p_t = 15$ GeV. Solid line: Born; dashed line: NLO

Fig. 2. π^0 production. p_t distributions of $\frac{d\sigma^{(ep)}}{d\eta dp_t}$ for different values of η_{lab}. **a)** Set I; **b)** Set II; **c)** Set III

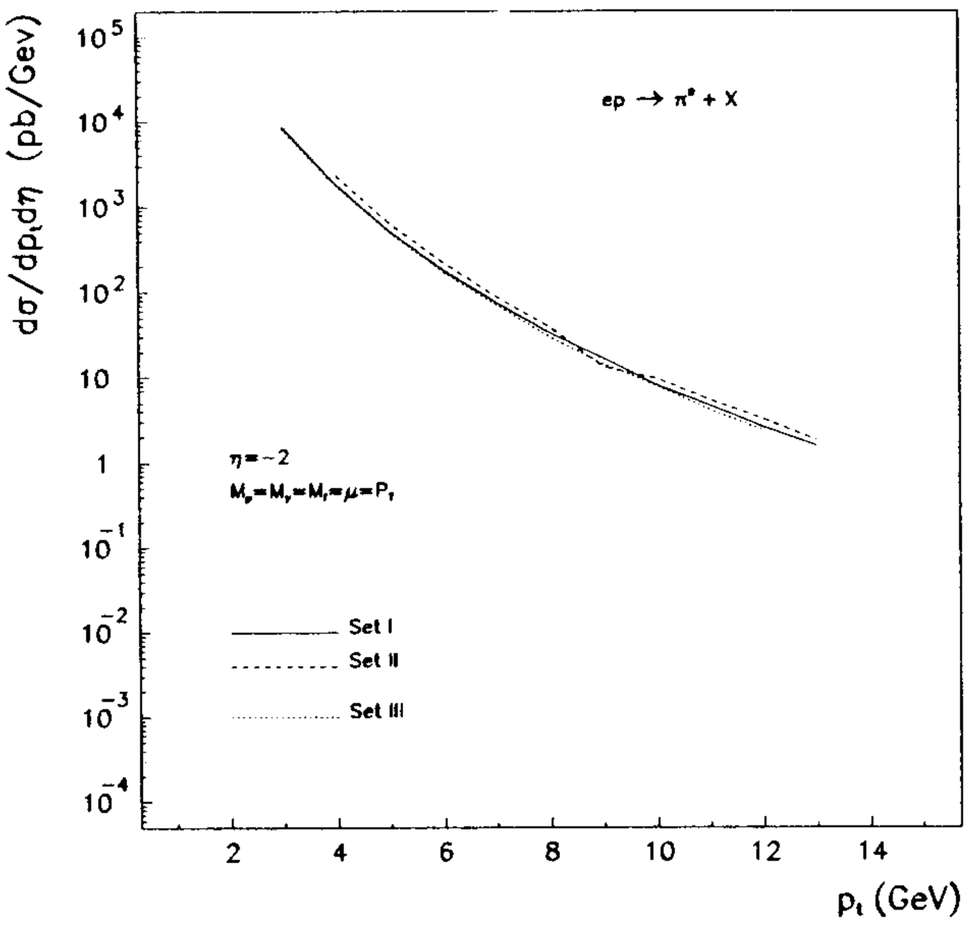

Fig. 3. π^0 production. p_t distributions of $\frac{d\sigma^{(ep)}}{d\eta dp_t}$ for $\eta_{lab} = -2$ for the three sets of photon structure functions

$$+\frac{1+(1-y)^2}{y}\ \log\frac{E^2(1-y)^2\theta_c^2+m_e^2y^2}{m_e^2y^2}$$

$$+\mathscr{O}(\theta_c^2, m_e^2/E^2)\Big\}, \qquad (4)$$

where $\theta_c = 5°$ is the maximum value of the electron scattering angle and m_e is the electron mass.

Finally the γp inclusive cross section is given by:

$$E\frac{d\sigma^{\gamma p}}{d^3P} = \frac{1}{\pi S}\sum_{i,j,l}\int_0^1\int_0^1\int_0^1 dx_1\ dx_2\ \frac{dx_3}{x_3^2}$$

$$F_i^p(x_1, M_p^2)F_j^\gamma(x_2, M_\gamma^2)D_l^h(x_3, M_f^2)\left(\frac{\alpha_S(\mu^2)}{2\pi}\right)^2$$

$$\left[\frac{1}{v}\sigma_{ijl}^0(s,v)\delta(1-w)\right.$$

$$\left.+\frac{\alpha_S(\mu^2)}{2\pi}K_{ijl}(s,v,w;M_p^2,M_\gamma^2,\mu^2,M_f^2)\right] \qquad (5)$$

where s, v and w are the partonic variables $s = x_1x_2S$, $v = \frac{x_2-1+V}{x_2}$, $w = \frac{x_2VW}{x_1(x_2-1+V)}$ and $V = 1+\frac{T}{S}$, $W = \frac{-U}{T+S}$, with S, T, U the hadronic Mandelstam variables. σ_{ijl}^0 are the partonic Born cross sections $O(\alpha_S^2)$, while K_{ijl} are the finite higher order corrections $O(\alpha_S^3)$ [3],with $i,\ j,\ l$ running on all kinds of partons.

As usual, the photon structure functions are expressed in terms of the hadronic and the pointlike contributions as $F^\gamma(x,Q^2) = F^\gamma_{had}(x,Q^2) + F^\gamma_{point}(x,Q^2)$, and obey the appropriate evolution equation with the inhomogeneous term related to F^γ_{point} [9].

As already stated above a consistent calculation to next-to-leading order needs two-loop evolved structure and fragmentation functions and a NLO evaluation of parton-parton subprocesses. In the partonic cross sections to one loop [3], calculated from the squared matrix elements $O(\alpha_S^3)$ of Ellis et Sexton [10], the initial state collinear divergences have been factorised and absorbed into the dressed structure functions in the $\overline{MS}$ scheme. Coherently with this choice, we have used for the proton structure functions set B1 of Morfin & Tung, [11] (set A), set MRS S0 of Martins, Roberts & Stirling [12] (set B), and set GRV HO of Glück, Reya & Vogt [13] (set C) and three different NLO parametrisations of the photon structure functions, namely the set of Aurenche et al. [14] with massless charm (set I), that of Glück, Reya and Vogt [15] (set II) (mode=272 in the PDFLIB library) and that of Gordon and Storrow [16] (set III). Sets I and II have been also used in the previous analysis of Borzumati et al. [2].

Table 1. Parameters of the $\pi^\pm$ fragmentation functions at $M_0 = 30$ GeV (see eq.6)

Parton	α	β	N_i	$< n_i >$
u	-1.14 ± 0.01	2.43 ± 0.03	1.09	5.15
d	-1.16 ± 0.01	2.26 ± 0.04	1.02	5.14
s	-0.90 ± 0.01	5.76 ± 0.06	2.93	4.91
c	-0.80 ± 0.01	7.52 ± 0.09	5.56	5.98
b	-1.14 ± 0.01	8.40 ± 0.06	2.37	7.41
g	-0.51 ± 0.01	5.02 ± 0.09	11.13	6.27

We have used α_S calculated at 2-loop, with 4 flavours and with $\Lambda_{QCD} = 200\ MeV$. Set A of the proton structure functions has been indeed evolved with $\Lambda_{QCD} = 194\ MeV$, but the error induced by this different choice is negligible. We have also considered 5 flavours in the proton, in the photon and in the final state, but the contribution given by the bottom is clearly negligible in the range of p_t values studied.

We have used the improved expression (4) for the Weizsäcker-Williams photon density in the electron [8]. When comparing our results with those obtained with the usual leading order formula (e.g. see eq.1 in ref. [17]) we found a negative correction which is not larger than 5%.

Fragmentation functions will be also considerd to NLO accuracy. For the π^0 case, various consistent parametrizations have been discussed in ref. [5], using different methods and initial conditions. All of them have been successfully compared with the current experimental data in e^+e^- and $p\bar{p}$ collisions at various energies. In the following we will use only one set of them, based on the MonteCarlo simulator HERWIG [18, 19], which is used to fix the initial conditions at the fragmentation scale $M_0 = 30$ GeV. The same method has also been applied in ref.[7] to inclusive η production, and indeed the predicted η/π^0 ratio has been found to agree with the present experimental information at ISR [20] and from e^+e^- and $p\bar{p}$ colliders. Recent fixed target experiments also agree [21] with the predictions of ref. [7]. We are therefore quite confident with the reliability of the method used and consequently we follow the same tecnique to obtain a new set of fragmentation functions NLO for $\pi^\pm$. The functions are parametrized as:

$$D_i^\pm(z, M_0^2) = N_i z^{\alpha_i}(1-z)^{\beta_i} \qquad (6)$$

where i runs over $(u,\ d,\ s,\ c,\ b,\ g)$, and $M_0 = 30$ GeV. The coefficients are given in Table 1 (we indicate the average multiplicity of produced hadrons with the symbol $< n_i >$).

We remark that we are considering the inclusive production of $(\pi^+ + \pi^-)$. We have used a new improved version of HERWIG, which also gives us a new π^0 fragmentation

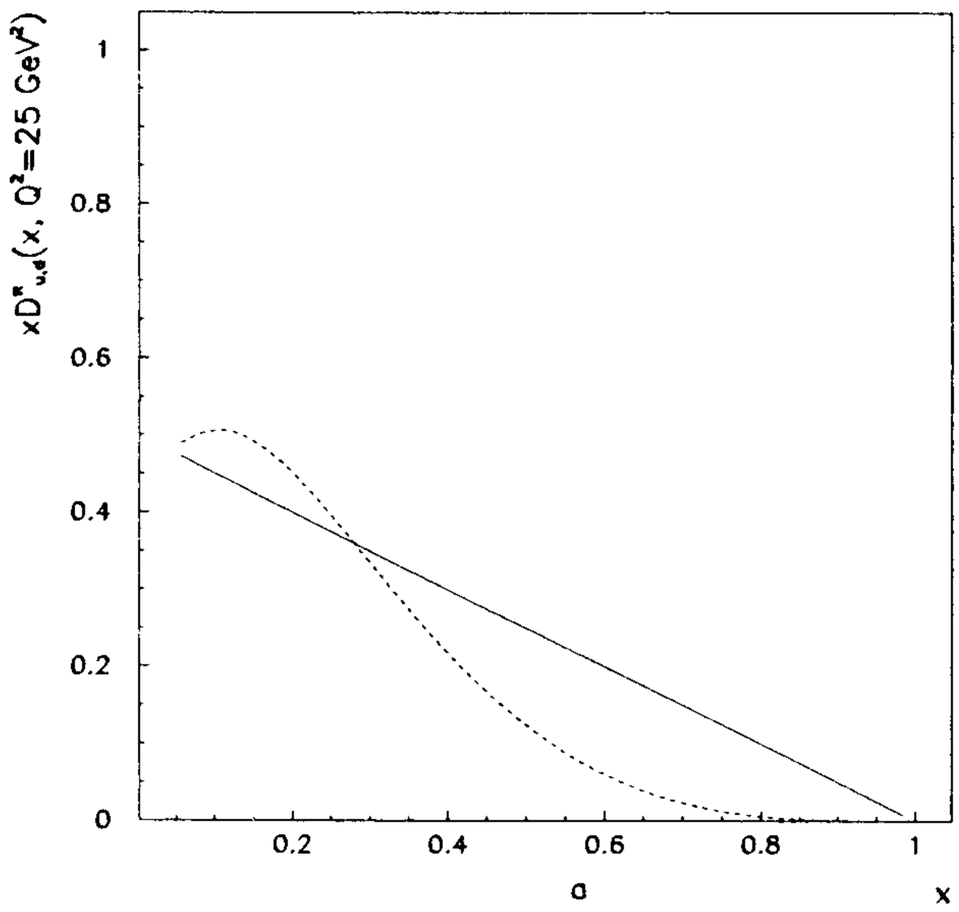

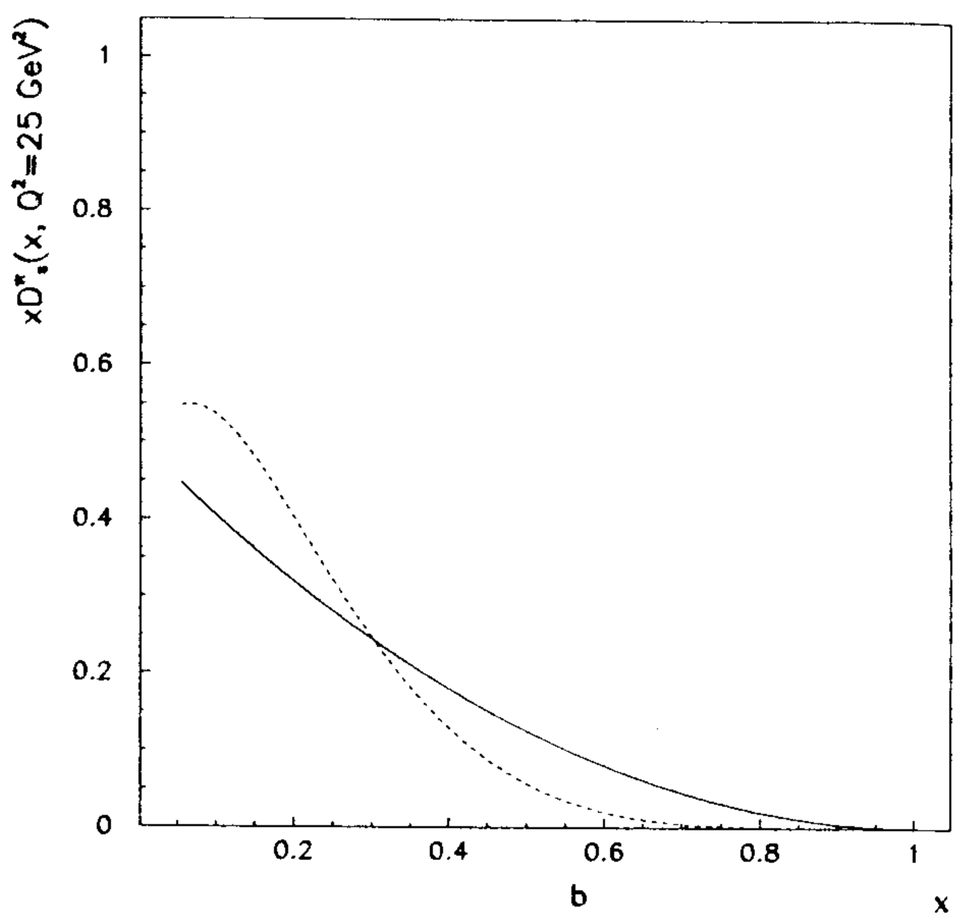

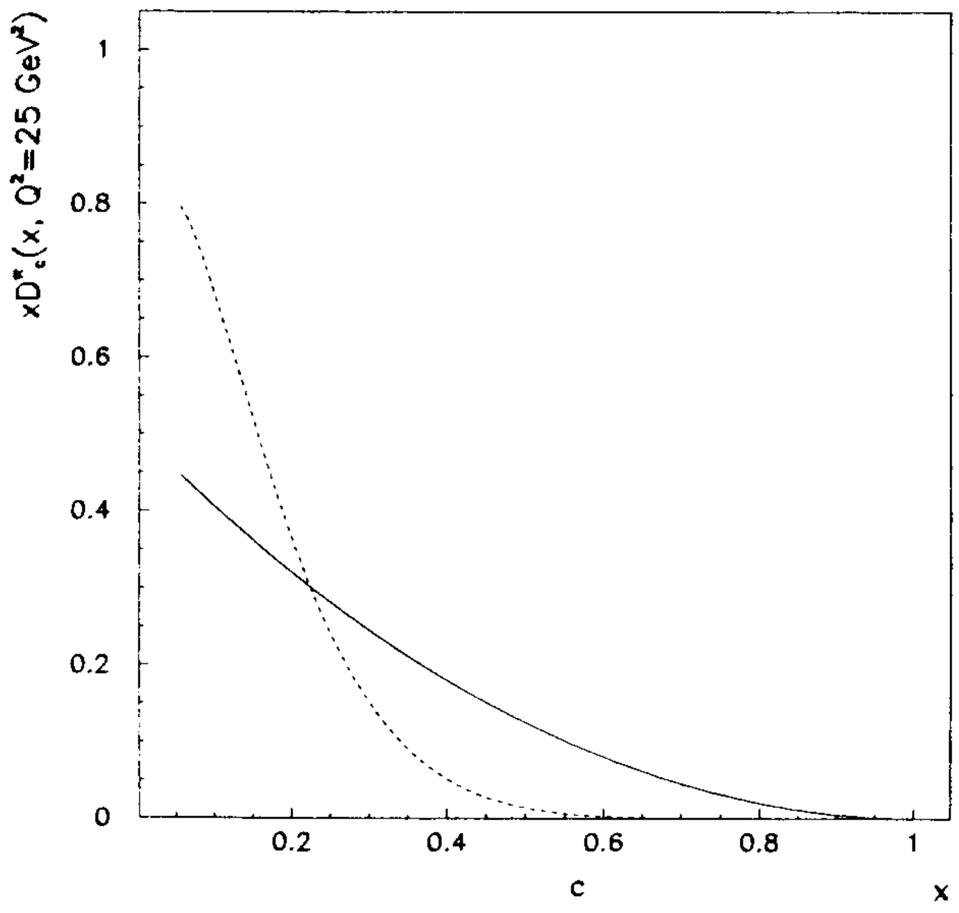

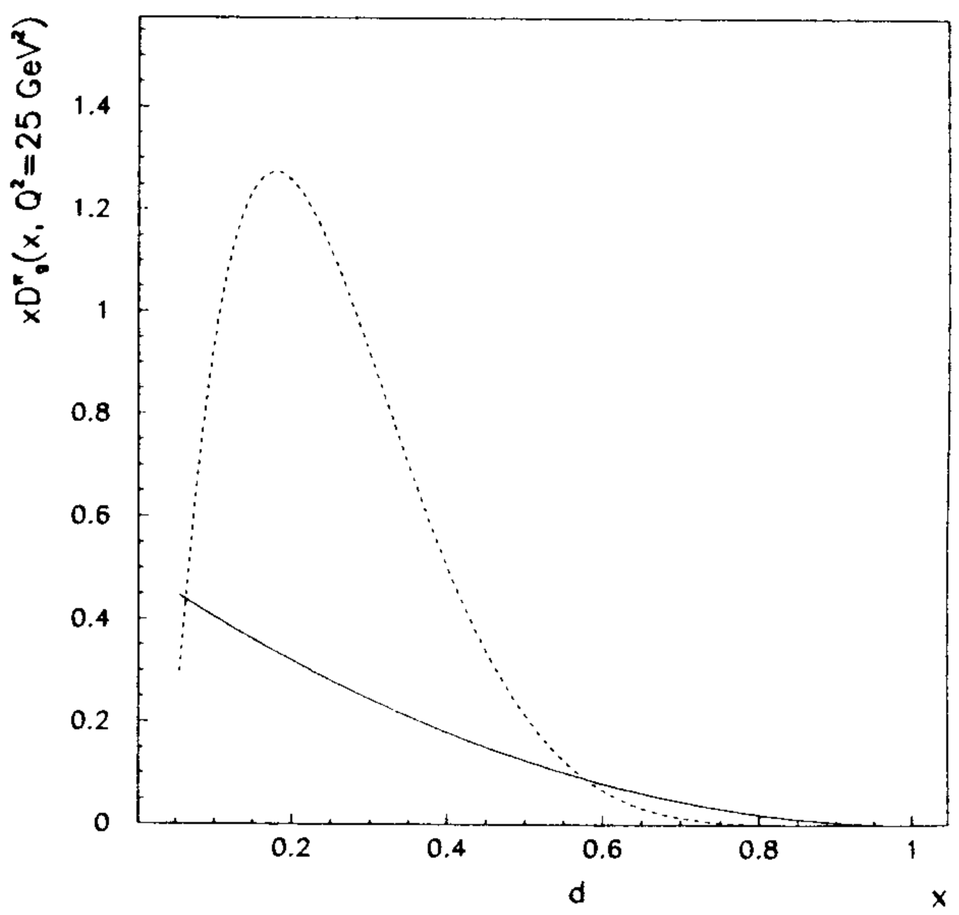

Fig. 4. π^0 fragmentation functions at $M_0^2 = 25$ GeV^2: continued line Herwig fragmentation functions, dashed line from ref [24]

set which is slightly different from that given in ref. [5], and actually improves the comparison with e^+e^- data at high z ($z > 0.7$). However, to the aim of the present work, the two sets of π^0 fragmentation functions based on the old and new versions of HERWIG are equivalent. For the sake of completeness we also give in Table 2 the new parametrization of π^0 quark fragmentation functions at $M_0 = 30$ Gev.

We present now various numerical results for the three sets of photon structure functions, studying in particular the uncertainties of the theoretical predictions. We always use set A for the proton and set I for the photon structure functions, except when explicitly mentioned. Let us consider π^0 photoproduction first.

The dependence of the cross section on the various mass scales involved in (5) is shown in Figs. 1. As expected, the dependence is very strong at the Born level, as shown in Fig. 1a for $p_T = 5\ GeV$, for $\eta_{lab} = -2$. The introduction of higher orders reduces the effect, although the dependence on the photon factorization scale only is still important (Figs. 1b-1c), unlike what is observed in the case of hadron-hadron collisions [3, 22]. This behaviour has been also observed in the photoproduction of jets at HERA [16, 23, 4], and the photon mass scale dependence is reduced when the direct and resolved terms are both considered [4]. The above

Table 2. Parameters of the quarks fragmentation functions into π^0 at $M_0 =$ 30 GeV (see text)

Parton	α	β	N_i	$< n_i >$
u	-1.18 ± 0.01	2.32 ± 0.05	0.53	2.83
d	-1.17 ± 0.01	2.41 ± 0.05	0.55	2.82
s	-0.94 ± 0.01	5.83 ± 0.08	1.46	2.66
c	-0.81 ± 0.01	9.01 ± 0.14	3.5	3.41
b	-1.35 ± 0.01	7.16 ± 0.07	1.25	4.19
g	-0.59 ± 0.01	4.43 ± 0.10	4.57	3.52

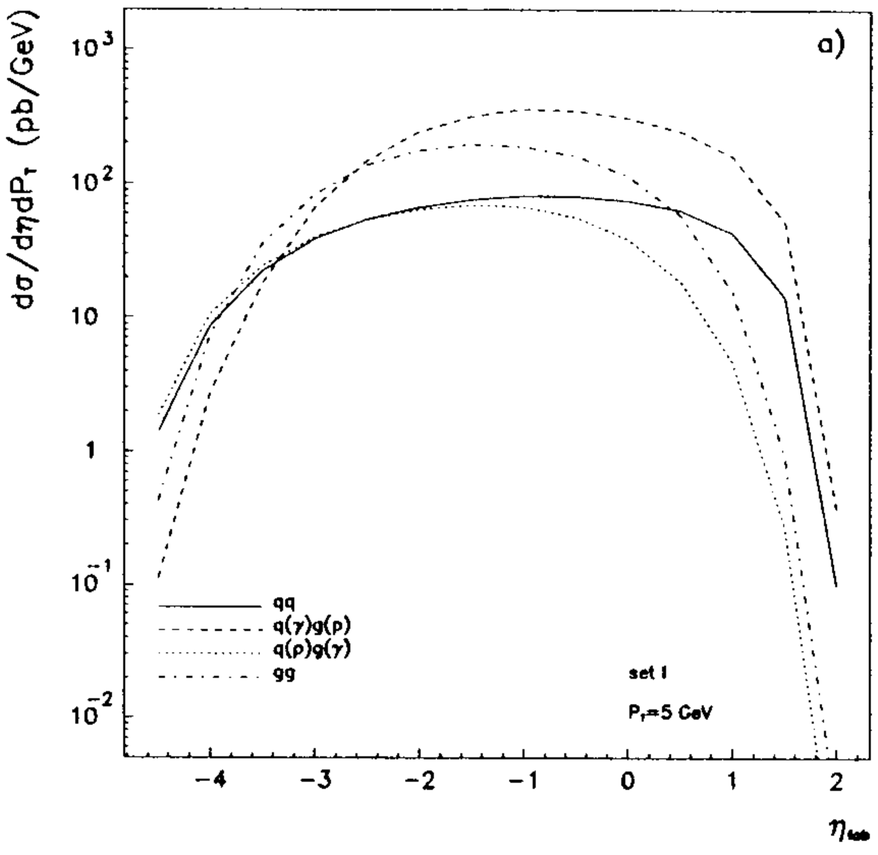

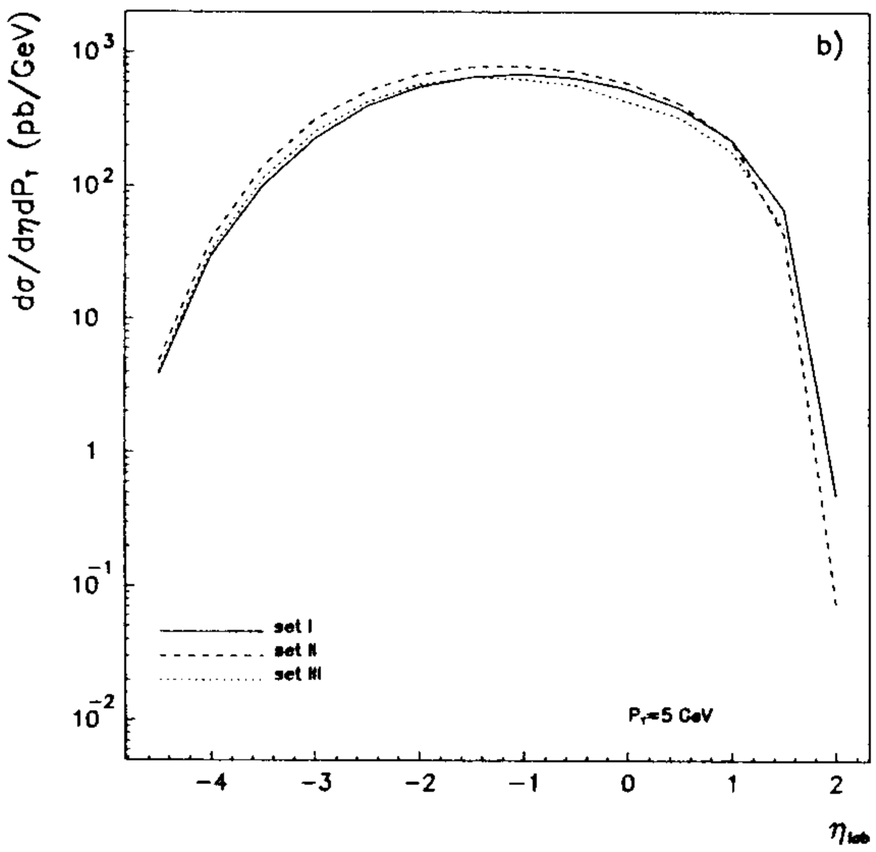

Fig. 5. π^0 production. η_{lab} distributions of $\frac{d\sigma^{(ep)}}{d\eta dp_t}$, for $p_t = 5$ GeV, for the partonic subprocesses: **a)** Set I; **b)** comparison of the total cross sections (sum of all the subprocesses) for the three sets

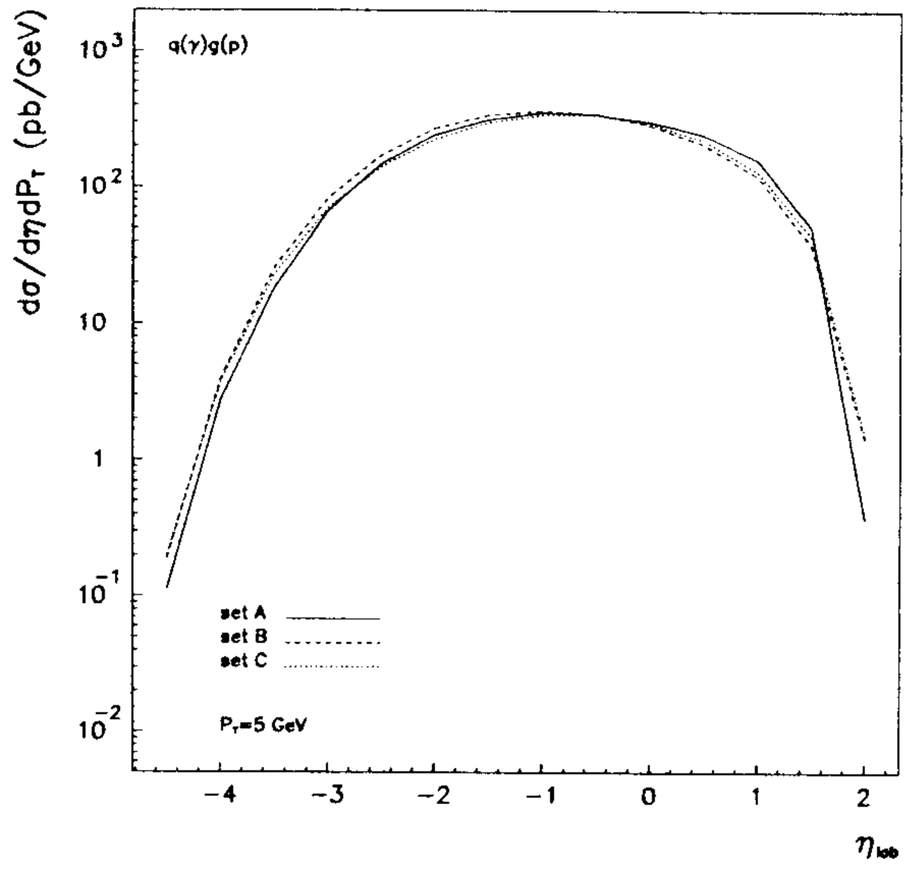

Fig. 6. π^0 production. η_{lab} distributions of $\frac{d\sigma^{(ep)}}{d\eta dp_t}$, for $p_t = 5$ GeV, for the subprocess $q(\gamma)g(p) \rightarrow \pi^0 + X$ for different sets of proton structure functions. Set I has been used for the photon structure function

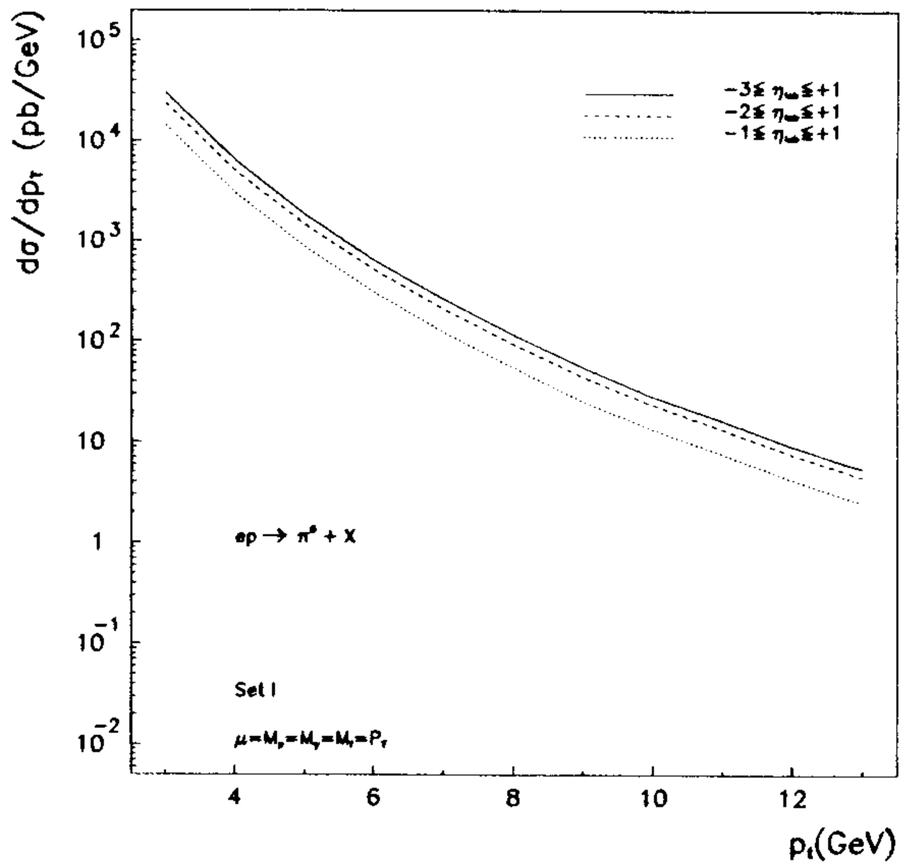

Fig. 7. π^0 production. p_t distributions of $\frac{d\sigma^{(ep)}}{dp_t}$ for different ranges of integrations over η_{lab}

effect is similar for the three sets of photon structure functions.

More explicitly we have isolated in the K factor in (5) the terms depending on M_p^2 from those depending on M_γ^2, with the following method. We split each term of the K-factors calculated in [3], which is proportional to $\log\left(\frac{s}{M^2}\right)$, where in [3] $M^2 = M_p^2 = M_\gamma^2$, in two pieces and assign a weight factor which takes into account the splitting vertex ($q \rightarrow qg$, $g \rightarrow gg$) present in the collinear emission. For the subprocesses $qq \rightarrow H+X$ and $gg \rightarrow H+X$ the weight is $\frac{1}{2}$, due to the simmetry of all possible collinear emissions. In the subprocess $q(p)g(\gamma) \rightarrow H+X$ and $q(\gamma)g(p) \rightarrow H+X$ we give a weight $\frac{C_F}{C_F+2C_A+n_F}$ to the quark and $\frac{2C_A+n_F}{C_F+2C_A+n_F}$ to the gluon (C_F and C_A are the usual color factors). Moreover for each subprocess one has to multiply the partonic cross-section for the appropriate combination of structure function.

In order to show the general p_T behaviour of the cross section, $\frac{d\sigma}{d\eta dp_T}$ is plotted in Figs. 2 and 3 for different values of η_{lab}, $\mu = M_p = M_\gamma = M_f = p_T$, and for the three sets. Comparing to the previous analyses of ref [2], we have found differences which we believe are essentially due to the use of our set of fragmentation functions evolved to NLO. On the other hand we are able to reproduce Fig. 9 of [2], using the same inputs, within a 15% of accuracy but with an almost identical shape. For convenience we show in Fig. 4 the comparison between the old set of fragmentation functions [24] and the one used in this paper [5].

In Figs. 5 we present the η_{lab} distribution for fixed $p_t = 5$ GeV. In Fig. 5a the contribution is shown by the various partonic subprocesses, while the differential cross-sections $\frac{d\sigma}{d\eta dp_T}$ for the three sets of photon structure functions are compared in Fig. 5b. Comparing with ref.[2], as for the case

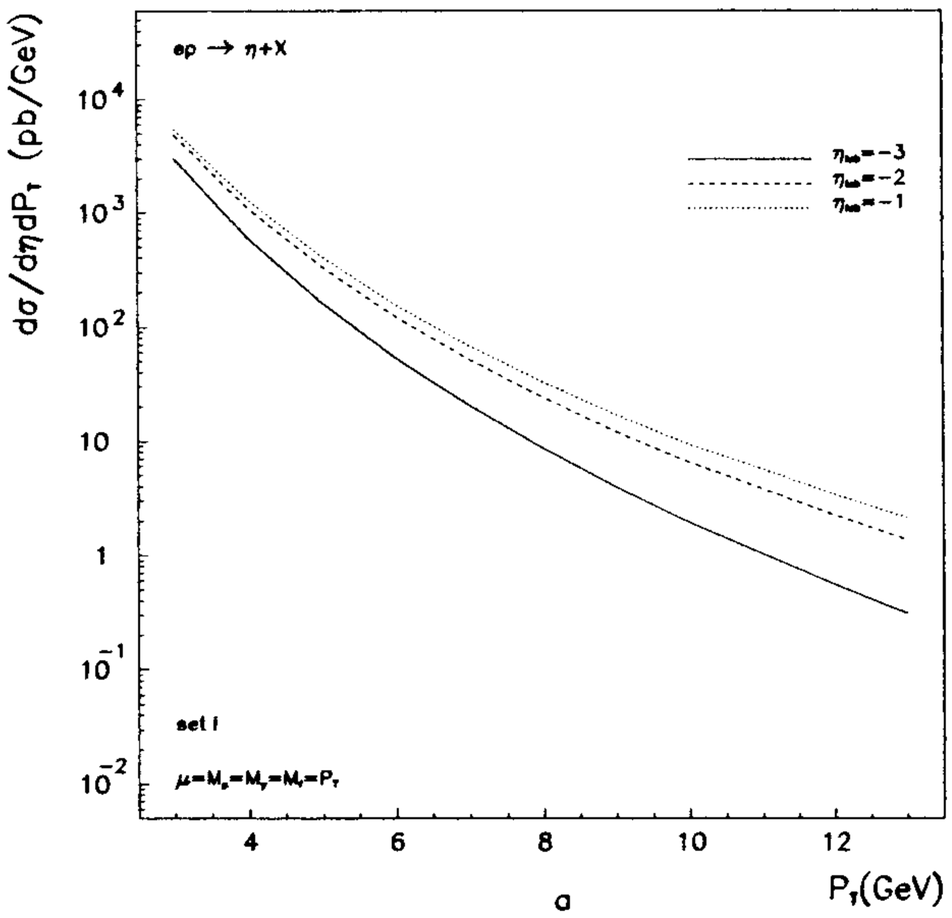

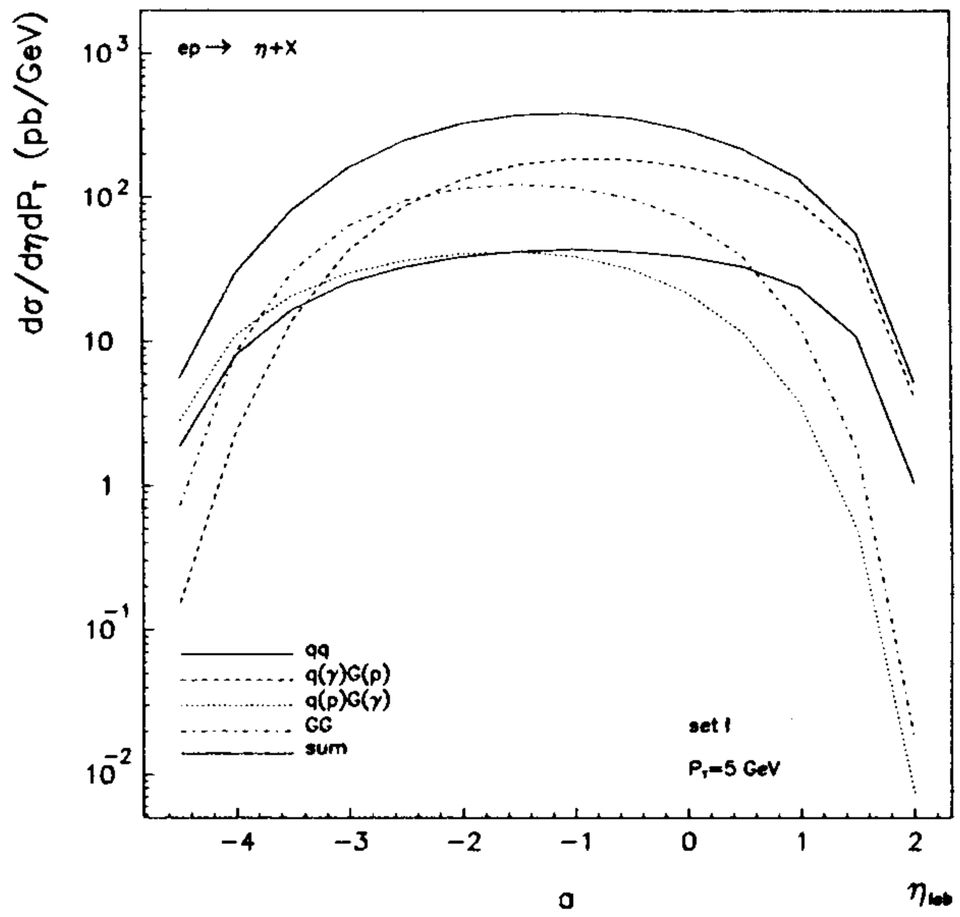

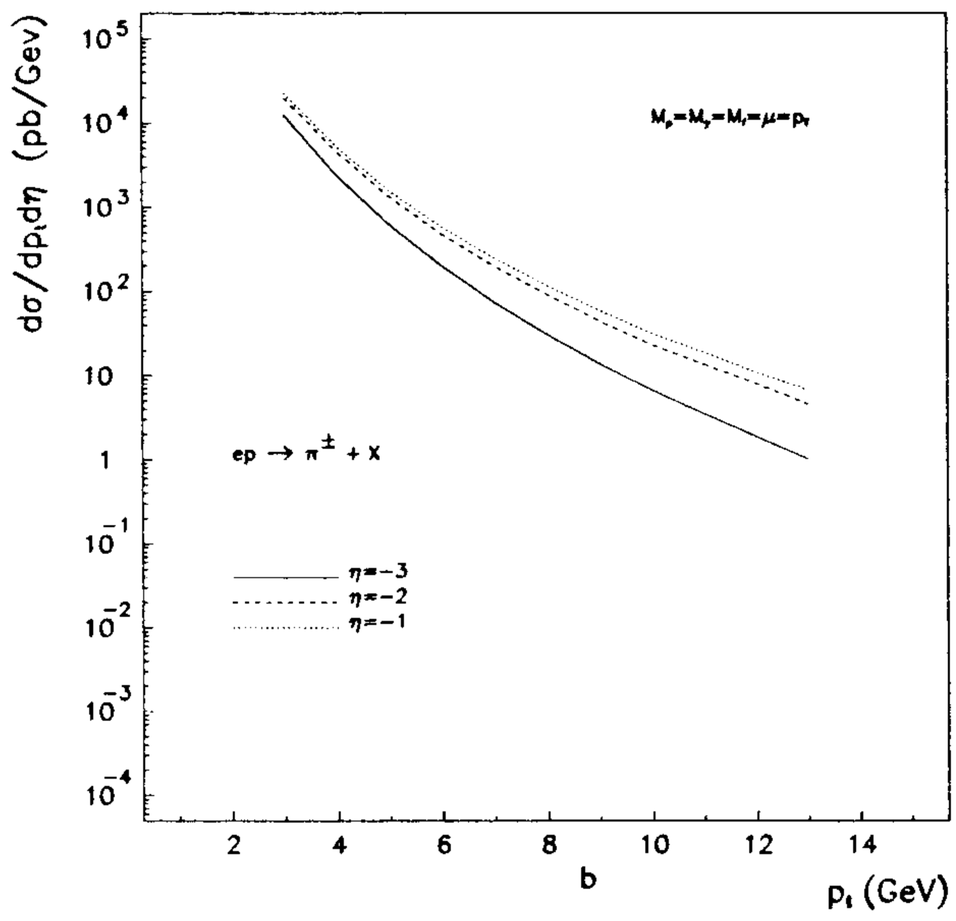

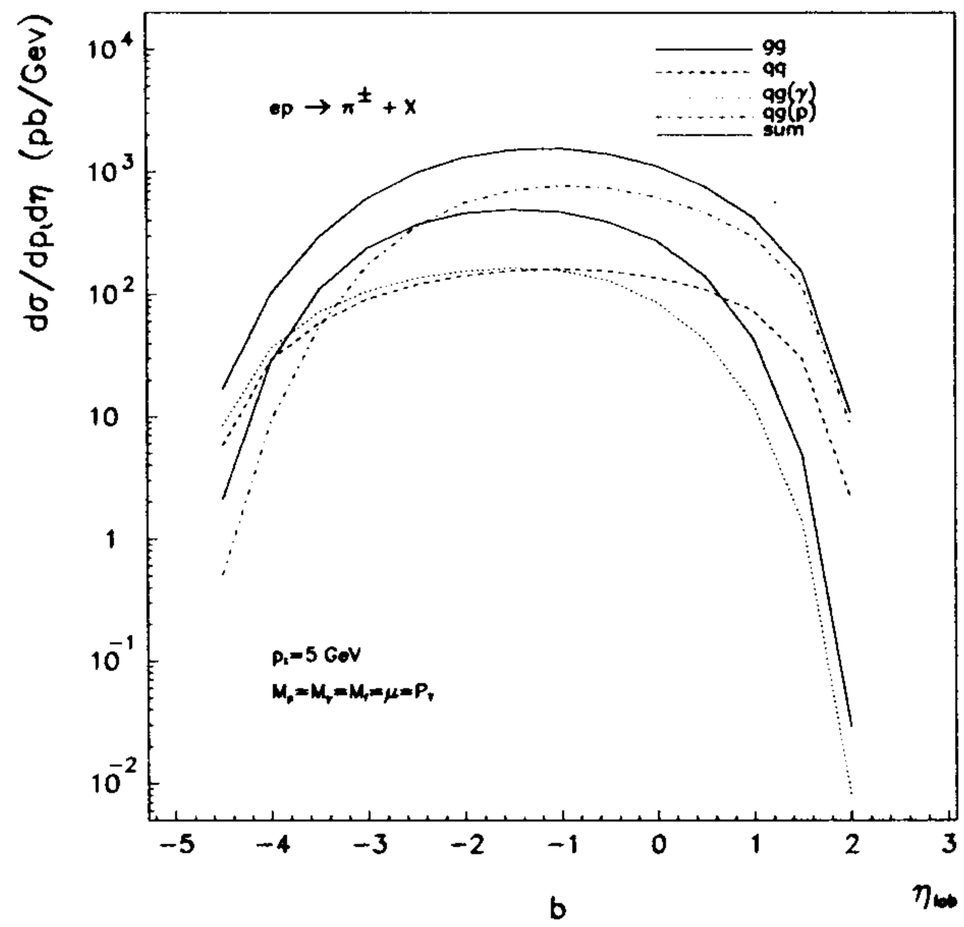

Fig. 8. p_t distributions of $\frac{d\sigma^{(ep)}}{d\eta dp_t}$ for $\eta_{lab} = -2$: **a)** $ep \to \eta + X$; **b)** $ep \to \pi^{\pm} + X$

Fig. 9. η_{lab} distributions of $\frac{d\sigma^{(ep)}}{d\eta dp_t}$ for $p_t = 5$ GeV: **a)** $ep \to \eta + X$; **b)** $ep \to \pi^{\pm} + X$

of p_t distributions, the different shapes shown in Fig. 5a can be understood firstly because of the different set of fragmentation functions (see Fig. 4); furthermore the regions $\eta_{lab} < -3$ and $\eta_{lab} > 1$ lie at the edge of phase space and therefore the numerical convolution of the $\gamma - p$ cross-section with the Weizsäcker-Williams formula is sensitive to slight variations of the parameters.

As in the case of inclusive jet photoproduction [4] the contribution from the gluon content of the photon is too tiny to be observed in most of the phase space available. Indeed from Fig. 5, if one considers the two subprocesses initiated by the gluon in the photon: $q(p)g(\gamma) \to jet + X$ and $gg \to jet + X$, the first one is clearly dominated by all other reactions, while the second one could be of interest in the region of very negative rapidities ($\eta_{lab} < -3$), where it is however quite difficult to disentangle the small-x behaviour of the photon structure function in the actual cross section.

On the contrary, the gluon contribution from the proton structure function plays a relevant role, and is essentially independent from the photon and proton structure functions, as also shown in Fig. 6, where the η_{lab} distribution of the subprocess $q(\gamma)g(p) \to \pi^0 + X$ for three different NLO parametrization of the proton structure functions.

We finally show the cross section integrated over different ranges of η_{lab} in Fig. 7, for the Set I of photon structure functions, which is of immediate phenomenological interest for HERA experiments.

Concerning the photoproduction of η and charged pions, we present in Figs. 8 the p_T distribution for different values of η_{lab}, in Figs. 9 the η_{lab} distributions for $p_t = 5$ GeV and for different subprocesses, and in Figs. 10 the distribution in p_t integrated in η_{lab}. The dependence on the photon structure functions is similar to what found for the π^0 case. Finally

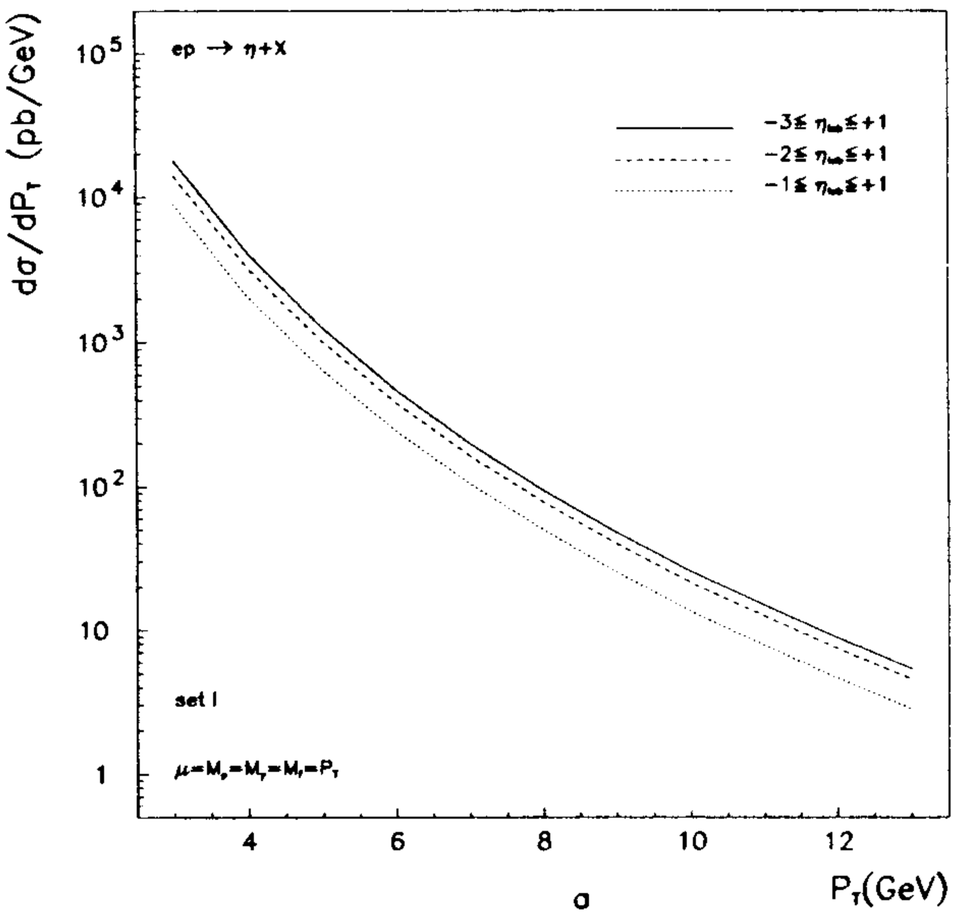

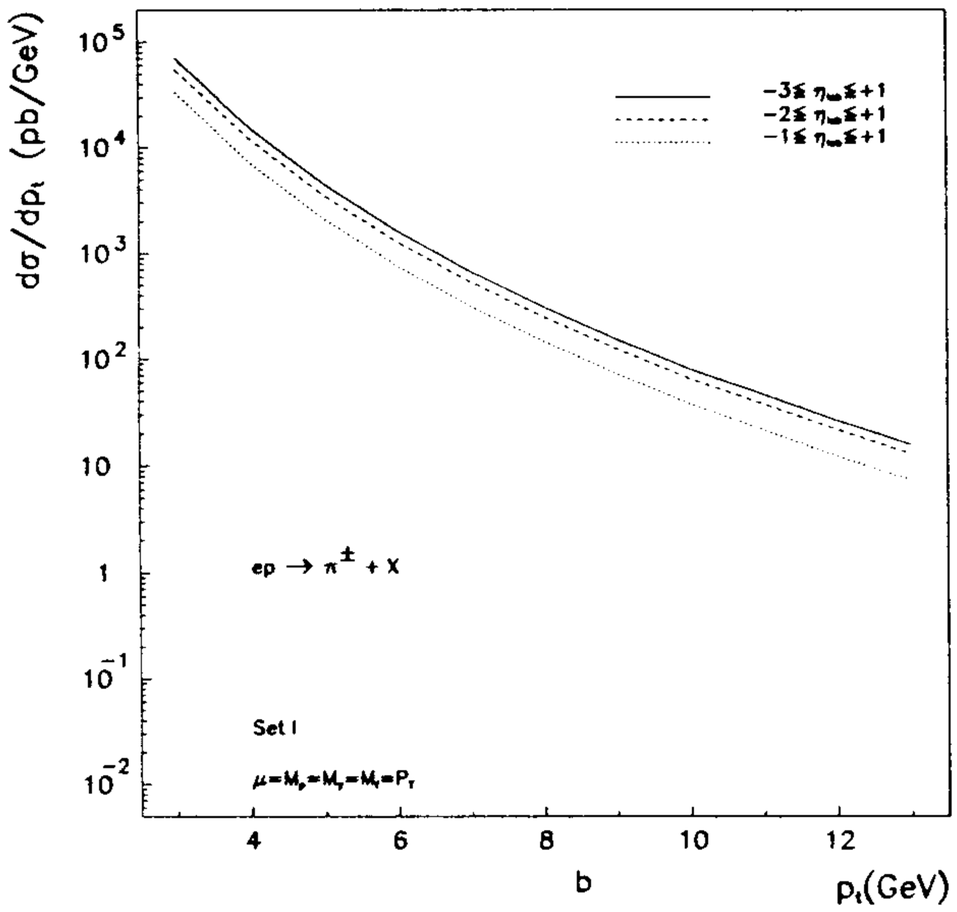

Fig. 10. p_t distributions of $\frac{d\sigma^{(ep)}}{dp_t}$ for different ranges of integrations over η_{lab}: **a)** $ep \to \eta + X$; **b)** $ep \to \pi^{\pm} + X$

we show in Table 3 our prediction for the ratio η/π^0 where we define R as the ratio of the cross sections $\frac{d\sigma}{d\eta dp_t}$ for the production of eta and pions respectively. In Fig. 11 we show the dependence of the cross section on the proton structure functions.

To conclude, a next-to-leading order calculation of inclusive neutral and charged pions and η production in electron-proton collisions has been presented, particularly via the resolved photon mechanism. We have studied the effects of the theoretical uncertainties related to the photon structure functions, as well as the dependence from the various mass scales, which is still significant in the considered p_t range. The inclusion of the direct component should make this effect weaker. We have also presented a new parametrization of $\pi^{\pm}$ fragmentation functions. Finally we stress that the gluon content of the proton can be accurately disentangled via the photoproduction of single particles at HERA.

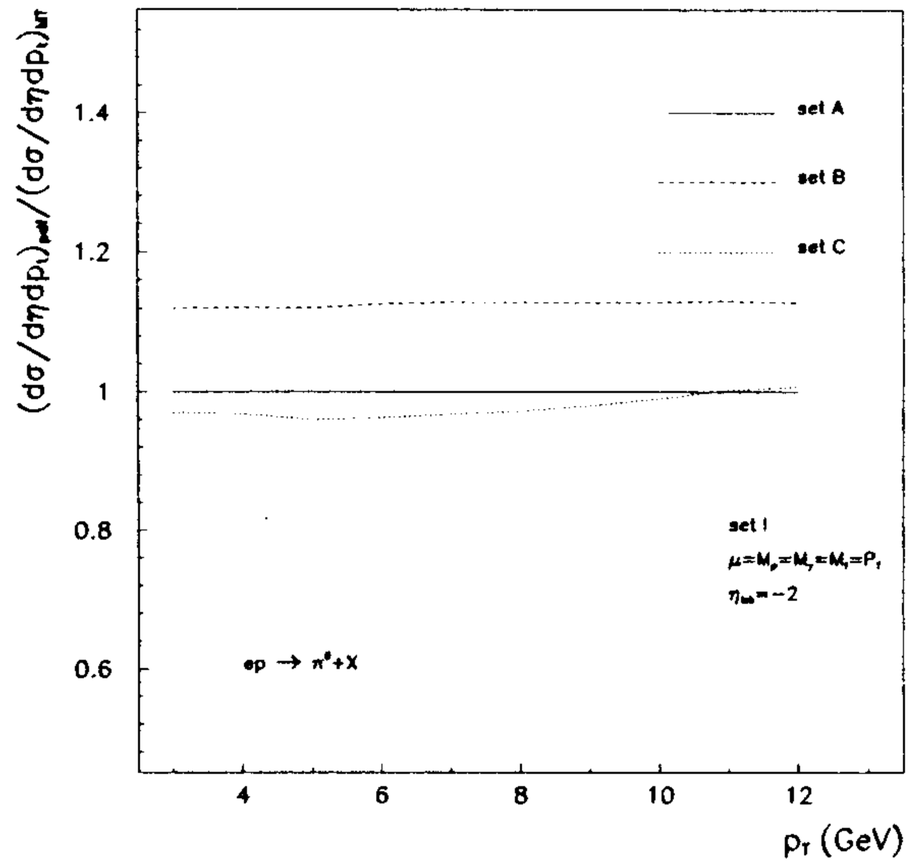

Fig. 11. π^0 production. p_t distributions of $ep \to \pi^0 + X$ for $\eta_{lab} = -2$ and set I for the photon structure functions; sets A, B and C are used for the proton structure functions (see text). Results are normalized to the calculation performed with Set A

Table 3. Ratio $R = \frac{d\sigma}{d\eta dp_t}(\eta) \Big/ \frac{d\sigma}{d\eta dp_t}(\pi^0)$ for different values of p_t and $\eta_{lab} 0 - 2$

$P_\perp$	R
3	0.55
4	0.60
5	0.64
6	0.67
7	0.67
8	0.72
9	0.72
10	0.79
11	0.80
12	0.84
13	0.86

When completing this work the paper "Inclusive particle production at Hera: resolved and direct quasi-real photon contribution in next-to-leading order QCD", by B.A.Kniehl and G.Kramer [25], has appeared, where a similar analysis has been carried out, including the direct photon contribution and using LO fragmentation functions. Direct comparison with the relevant figures of [25], using the same structure and fragmentation functions inputs, shows an overall agreement within 15-20%.

Acknowledgements. We thank Giovanni Abbiendi for providing us the new version HERWIG57, when it was also in a preliminary phase. This work was supported in part by the DOE and by the NASA (NAGW-2831) at Fermilab.

References

1. P.Aurenche et al.; Nucl.Phys. B 286 (1987) 553.
2. F. M. Borzumati, B. A. Kniehl, G. Kramer; Z.Phys. C 59 (1993) 341.
3. F.Aversa, P.Chiappetta, M.Greco and J.Ph.Guillet; Nucl.Phys.B327 (1989) 105.
4. M. Greco and A. Vicini; Nucl. Phys. B 415, 386 (1994)

5. P. Chiappetta, M. Greco, J. Ph. Guillet, S. Rolli, M. Werlen; Nucl. Phys. B 412 (1994) 3.
6. Work in progress.
7. M. Greco and S. Rolli; Z.Phys. C 60 (1993) 169.
8. S. Frixione, M. Mangano, P. Nason, G. Ridolfi; Phys. Lett. B 314 (1993) 339.
9. E. Witten, Nucl. Phys. B 120 (1977) 189.
10. R.K.Ellis and J.C.Sexton; Nucl.Phys.B 269 (1986) 445.
11. J.G.Morfin and Wu-Ki Tung; Z.Phys. C 52 (1991) 13.
12. A. D. Martin, R. G. Roberts, W. J. Stirling; Phys. Rev. D 47 (1993) 867.
13. M. Glück, E. Reya, A. Vogt; Z.Phys. C 53 (1992) 127
14. P.Aurenche, P.Chiappetta, M.Fontannaz, J.Ph.Guillet and E.Pilon; Z.Phys. C 56 (1992) 589.
15. M.Glück, E.Reya and A.Vogt; Phys.Rev. D45 (1992) 3986.
16. L.E.Gordon and J.K.Storrow; Phys.Lett. B 291 (1992) 320, L.E.Gordon and J.K.Storrow Z.Phys. C 56 (1992) 307.
17. H.Baer, J.Ohnemus and J.F.Owens; Z.Phys. C 42 (1989) 657.
18. G. Marchesini, B.R. Webber; Nucl Phys. B 238 (1984) 1.
19. G. Marchesini, B.R. Webber; Nucl Phys. B 310 (1988) 461.
20. F. Büsser at al; Nucl. Phys. B 106 (1976) 1.
21. E706 Collaboration; talk given at Moriond 94.
22. R.K.Ellis,P.Nason and S.Dawson; Nucl.Phys.B 303 (1988) 724.
23. G. Kramer and S. G. Salesch; Z.Phys. C 61 (1993) 277.
24. R. Baier, J. Engles, B. Petersson: Z. Phys. C 2 (1979) 265; M. Anselmino, P. Kroll, E. Leader: Z. Phys. C 18 (1983) 307.
25. B. A. Kniehl and G. Kramer; DESY 94-009, Z. Phys. C (1994)